Synthesis and characterization of nanostructured CeO$_2$ with dyes adsorption property

Oman Zuas[1],*, Haznan Abimanyu[1], Widayanti Wibowo[1]

[1]*Research Centre for Chemistry, Indonesian Institute of Sciences (RCChem-LIPI), Kawasan PUSPIPTEK Serpong, 15314, Tangerang, Banten, Indonesia*
[2]*Department of Chemistry, Faculty of Mathematics and Natural Science, University of Indonesia, Kampus UI Depok 16424, Depok, Indonesia*

Abstract

The nanostructured cerium dioxide (CeO$_2$) has been successfully fabricated using a simple precipitation method. Its characteristics were evaluated using TG-DTA, DR-UV-Vis, XRD, FTIR and TEM. The results showed that the nanostructured CeO$_2$ has high purity and good crystalline nature, with face centered cubic (fcc) phase and the average diameter of CeO$_2$ single crystal about 14 nm. Performance evaluation of the synthesized CeO$_2$ samples showed that the nanostructured CeO$_2$ has a strong adsorption toward acid orange-10 (AO-10) and congo red (CR) in aqueous solution. Under given experimental conditions (dye concentration of 15 mg/l, adsorbent dosage of 1 g/l, reaction temperature of 30 ± 1 °C), it was estimated that the adsorption equilibrium for AO-10 and CR occurred at 60 min and 90 min of reaction time, respectively, with total removal of 96.82 % for AO-10 dye and 93.55 % for CR dye. The results suggested that the CeO$_2$ nanopowder could be potentially used as an efficient adsorbent for the removal of synthetic organic dyes in aqueous solution and may address for future concern in the area.

Keywords: nanostructure, CeO$_2$, congo red, acid orange 10, adsorption

I. Introduction

Synthesis of nanostructured metal oxides having tremendous physical and chemical properties (which are usually significantly different from their bulk particles) has attracted considerable interest in both academic and research. Cerium dioxide (CeO$_2$), is one of the most important metal oxide in daily life and has been used in wide area of applications. In industrial field, the CeO$_2$ has been used as an additive in ceramic manufacture [1]. CeO$_2$ was also reported as a promising catalyst with high catalytic performance for organic chemical synthesis [2]. For UV hazard protection, CeO$_2$ has been reported as an effective material for UV blocking material [3] and sunscreen cosmetic [4]. CeO$_2$ was also found as an alternative solid electrolyte for fuel cell for energy saving purposes [5–7]. In the field of environ-

mental protection and remediation, CeO$_2$ has been reported as active materials for controlling automotive exhaust emission, as photocatalyst/catalyst for the degradation of chemical pollutant, and as highly-efficient absorbents for dyes removal [8–12].

Synthesis of CeO$_2$ having nano dimensional structures was firstly reported by Matijević and co-workers in 1987 [13]. Since then, a number of methods for the synthesis of nanostructured CeO$_2$ have been reported in published literatures including microwave-assisted [14], sol-gel [15], ultrasonication [16], hydrothermal [17,18], precipitation/co-precipitation [2,19] and micro emulsion method [20]. Among these synthesis methods, precipitation/co-precipitation method is preferred because it is inexpensive, relatively simple, and CeO$_2$ powder having crystal size on nano scale could be obtained. It is widely acceptable idea that synthesis of nanostructured metal oxide is generally designed to achieve an active material that is otherwise not reactive.

Regarding to the aqueous environmental-related is-

*Corresponding author: tel: +62 21 7560929,
fax: +62 21 7560549, e-mail: *oman.zuas@lipi.go.id*,
oman.zuas@yahoo.co.id

sues, water pollution by synthetic dyes from industries such as textiles, paper, and plastic might be one of the most serious problems. It has been reported that hundred thousand tonnes of commercial dyes are produced annually [21,22] and they are used by industries to colour their product [23]. Water pollution by synthetic dyes can be occurred because high percentage of coloured industrial effluents is discharged directly into aqueous environment [24,25]. The presence of coloured dye effluents in aqueous environment can potentially threat the aqueous ecosystem because they are aesthetic pollutants, resistant to aerobic digestion, stable to light heat and oxidizing agents, and they can hinder the light penetration required for the aqueous biological processes [26–28]. In addition, the coloured effluents may contain some harm chemicals that are toxic, carcinogenic, or mutagenic for the aquatic life [26,28,29]. Therefore, an action to remove the dyes from industrial wastewater before being discharged into the aqueous environmental is essential. There are some conventional treatment technologies for dyes removal have been reported including chemical coagulation, anaerobic reduction, aerobic oxidation, membrane filtration, photo-degradation and adsorption methods [23,27,28,30,31]. Among the reported technologies, the adsorption process provides an attractive method especially if the adsorbent has high adsorption property and recyclable.

Thus, this study is not only aimed to synthesis the nanostructured CeO_2 using a simple precipitation method but also to evaluate its activity. The activity of the synthesized CeO_2 was evaluated as material absorber for removal of synthetic organic dye in aqueous solution. The structural and morphological of the synthesized CeO_2 were evaluated using thermogravimetry-differential thermo analysis (TG-DTA), diffuse reflectance-UV visible (DR-UV-Vis) spectroscopy, X-ray diffractometry (XRD), Fourier transform infrared spectroscopy (FTIR), and transmission electron microscopy (TEM). The environmental activity of the synthesized CeO_2 was evaluated as an adsorbent for removal of dyes pollutant from water.

II. Experimental details

All chemicals were analytic grade and used as received without further purification. Cerium (III) nitrate hexahydrate ($Ce(NO_3)_3 \times 6H_2O$, 98 % purity, Merck, Germany), aqueous ammonia solution (NH_4OH, 25 % purity, Merck, Germany), N-Cetyl-N,N,N-trimethylammonium bromide (*CTAB*, 98 % purity, Merck, Germany), congo red dye ($C_{32}H_{22}N_6O_9S_2Na_2$, C.I. 22120, CAS No. 573-58-0, Sigma-Aldrich, Germany), and acid orange 10 dye ($C_{16}H_{10}N_2O_7S_2Na_2$, C.I. 16230, CAS 1936-358-4, Sigma-Aldrich, Germany). The molecular structure of AO-10 and CR are presented in Figs. 1a and 1b, respectively. Double distilled water was used in all the experimental runs.

The nanostructured CeO_2 was synthesized using a simple precipitation method adopted from literature [32]. In a typical experiment, an appropriate amount of $Ce(NO_3)_3 \times 6H_2O$ was dissolved into 500 ml CTAB (0.02 M) solution to give 0.12 M of $Ce(NO_3)_3 \times 6H_2O$ in the mixture solution. The mixture solution was precipitated using NH_4OH solution under vigorous stirring until the pH 10 of the mixture solution was reached. The coloidal solution formed was aged at 55–60 °C for 6 h followed by centrifugation at 8000 rpm for 10 min to remove the supernatant. Wet solid material obtained was then washed thoroughly with copious amount of double distilled water and then dried at 100 °C for 12 h to produce dry solid materials (referred to as-synthesized sample). The as-synthesized sample were ground in an agate mortar and calcined at 500 °C for 4 h in open air in a tube box muffle furnace to obtain the nanostructured CeO_2.

The as-synthesized sample was subjected to thermal (TG-DTA) analysis on a TGA DuPont 951 in the presence of static air at a heating rate of 10 °C/min from 25–1000 °C. Diffuse reflectance-UV visible (DR-UV-Vis) spectra were recorded on a Shimadzu UV2450 spectrophotometer under ambient temperature and $BaSO_4$ was used as a reference. X-ray diffraction (XRD) pattern of the CeO_2 nanopowder was recorded on a Philips-Type PW1710 X-ray diffractometer with Cu (λ = 1.5406 Å) irradiation and scanned 2θ in the range of 10–80° at a scanning speed of 1.2°/min. Fourier transform infrared (FT-IR) spectra were recorded with a FTIR-2000 Perkin Elmer using KBr plate at room temperature in the range of 500 to 4000 cm⁻¹ with scanning rate of 4 cm⁻¹/min. Transmission electron microscopy (TEM) micrographs were recorded on a Philip CM30

| (a) | (b) |
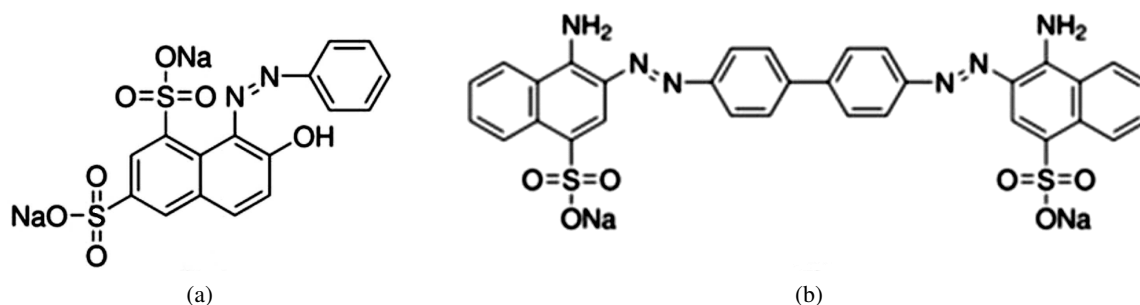
Figure 1. Molecular structure of: a) AO-10 and b) CR dyes

TEM operated at 200 kV. The CeO_2 nanopowder for TEM observation was dispersed in ethanol, sonicated and then very small amount of the suspension was deposited onto a 300 mesh copper grid.

Activity of the synthesized CeO_2 was evaluated as an adsorbent for the removal of AO-10 and CR in aqueous solution. The adsorption experiments were conducted in a 50 ml capped glass tubes containing 50 ml of dyes solution (15 mg/l) and certain amount of CeO_2 nanopowder (1 g/l). The sample-containing glass tubes were shaken in a Certomat WR-Braun Biotech International temperature-controlled water bath shaker with a constant agitation speed (140 rpm) and 30 ± 1 °C. Periodically, 5 ml of testing solution was taken. The dye filtrates were separated from the solid adsorbent material by centrifugation. Absorbance of the filtrates was then measured using a Hitachi U-2000 UV-Vis spectrophotometer at wavelength maximum of the dyes (λ_{max} = 480 nm for AO-10 and λ_{max} = 500 nm for CR). The concentrations of the dyes that remain in the sample solution were calculated from a calibration curve. The percentage adsorption was calculated using Eq. 1 below.

$$\% \text{Adsorption} = \frac{C_0 - C_t}{C_0} \cdot 100 \qquad (1)$$

where C_0 (mg/l) and C_t (mg/l) are the initial concentration and concentration of dye after time t, respectively.

III. Results and discussion

TG-DTA is an essential laboratory instrument used for material characterization. In TG-DTA experiment, properties of materials is monitored as a function of temperature in a controlled atmosphere as they change with temperature. TG-DTA profiles of the as-synthesized sample are depicted in Fig. 2. The TG curve of the as-synthesized sample under static air showed three main steps of weight losses (Fig. 2a). At the first step, the weight loss of 9.05 % occurs below 130 °C. Secondly, the weight loss of 14.79 % with a broad endothermic peaks is observed in the temperature ranging from 200 to 500 °C. At the third step, a little change in the mass of sample in the TG curve is observed at temperature above 500 °C with 1.49 % weight loss. The first step can be attributed to the release of adsorbed water, while the second step could be attributed to the dehydroxylation of the sample surface and loss of surfactant template. The third step could indicate the completion of any reaction involving removal of very little residual surfactant. From these TG results, it is obvious that most of the surfactant in the as-synthesized sample was eliminated at about 500 °C. Thus, the calcination of the as-synthesized sample in open air has been performed at 500 °C. The DT curve of the as prepared sample is shown in Fig. 2b. There are four exothermic peaks centered at about 135, 290, and 500 °C. The first two exothermic peaks represent the desorbtion of water and dehydroxylation of the sample surface, respectively.

While the exothermic peak at about 500 °C is associated with the loss of surfactant and starting the formation of crystalline CeO_2.
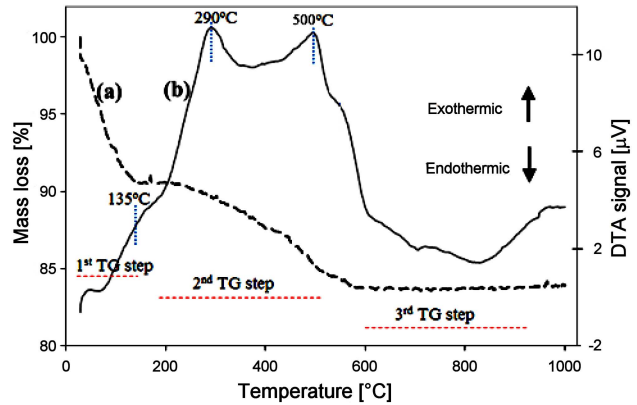
Figure 2. Profiles of: a) TG, and b) DTA of as-prepared sample heated in the presence of static air with a ramp rate of 10 °C/min
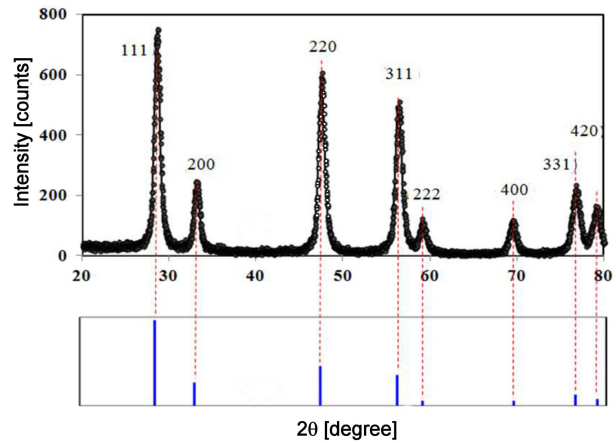
Figure 3. XRD pattern of the nanostructured CeO_2 calcined at 500 °C (with peak intensities according to JCPDS Card No. 43-1002)

Phase and purity of the CeO_2 nanopowder was evaluated by the XRD analysis and the result is shown in Fig. 3a, and for comparison the CeO_2 standard JCPDS Card No. 43-1002 is also included. The CeO_2 nanopowder (Fig. 3a) revealed diffraction peaks (2θ) at about 28.63°, 33.05°, 47.53°, 56.41°, 59.07°, 69.45°, 76.77°, and 79.19° which are ascribed to the 111, 200, 220, 311, 222, 400, 331, and 420 planes, respectively. All these diffraction peaks are in good agreement with the XRD pattern of the the CeO_2 standard (JCPDS Card No. 43-1002), that are indexed as a face centered cubic (*fcc*) phase.

No impurity phases can be observed, indicating high purity of the nanostructured CeO_2. The average crystallite size of the photocatalyst samples were calculated from the full-width at half-maximum (FWHM) of 111 reflection as presented in Fig. 3a using Scherrer's formula as shown in Eq. 2 [33]:

$$D = \frac{0.9\lambda}{\beta \cos \theta} \qquad (2)$$
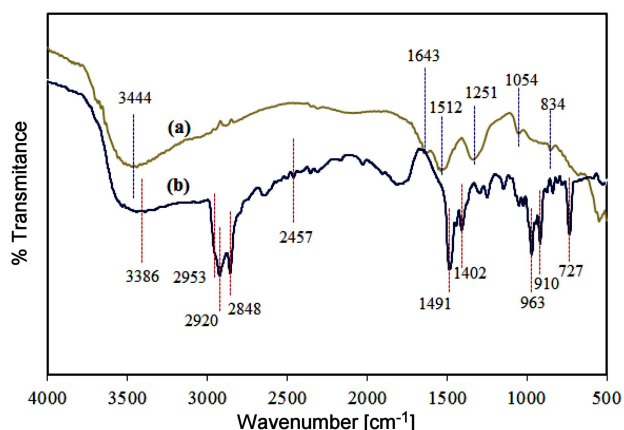
Figure 4. FT-IR spectra of: a) the as-synthesized sample and b) the nanostructured CeO$_2$ calcined at 500 °C

where D is the crystallite size, λ is the wavelength of the X-ray diffraction, β is the FWHM, θ is the angle of diffraction. It was obtained that the average diameter of the CeO$_2$ crystal was about 14.5 nm. In addition, well-defined peaks of the XRD diffraction confirm that the nature of the nanostructured CeO$_2$ were formed in good crystal quality.

Figure 4 presents the FT-IR spectra of the as-synthesized and the nanostructured CeO$_2$ after calcination at 500 °C. As can be seen from the as-synthesized sample (Fig. 4a) that the presence of surfactant CTAB is marked by the bands at 3386, 2920, 2848, 2457, 1491, 1402, 963, 910, 727 cm^{-1}. Some of these peak positions have slightly shifted to higher wavenumber compared to that of CTAB bands found in literature which was probably due to the interaction of CTAB with CeO$_2$ crystals and solvent during synthesis [34,35]. The adsorption band around 3384 cm^{-1} is attributed to the O–H vibration in absorbed water on the sample surface. The existence bands around 2953 cm^{-1} and 2848 cm^{-1} are indicative of –CH$_3$ stretching vibration.

In addition, the vibrational bands of –CH$_2$ are ob-

served at around 2920 cm^{-1} and 2457 cm^{-1}. The absorption band around 1491, 963 and 910 cm^{-1} are assigned to the vibrational band of –CH$_3$ from tertiary amine in CTAB, while the band at around 1402 cm^{-1} and 727 cm^{-1} are attributed to the –CH$_2$ vibration of tertiary amine. These CTAB bands become weaker or disappear in the FT-IR spectrum of the nanostructured CeO$_2$ after calcination at 500 °C (Fig. 4b), indicating the CTAB has been eliminated from the calcined CeO$_2$ sample. On the other hand, some typical bands of the CeO$_2$ can be observed in Fig. 4b. The FT-IR peaks positions of the CeO$_2$ nanopowder were found at about 1512, 1251, 1054, and 834 cm^{-1} that are similar to the FTIR bands of CeO$_2$ as reported literature [36,37]. At band below 700 cm^{-1}, the stretching frequency of Ce–O can also be obviously observed [36].

The TEM images were taken for morphological evaluation of the nanostructured CeO$_2$ (Fig. 5). Observation of the bright-field image (Fig. 5a) displays that the nanostructured CeO$_2$ crystal were formed with non-uniformity of spherical shape. From the high resolution TEM image of the nanostructured CeO$_2$ crystal, shown in Fig. 5b, it is obviously observed the grain boundary of the CeO$_2$ with a clear crystal diameter. The crystal diameter was estimated ranging from 10 to 16 nm. The lattice fringes observed (inset of Fig. 5b) indicates that the crystal of the nanostructured CeO$_2$ are presence in good quality nature [38]. The data from the TEM observation are in agreement with the XRD results.

The light absorbance characteristics of the synthesized samples in the UV-visible range were investigated from the diffuse reflectance spectra. The measured reflectance spectra obtained were transformed into Kubelka-Munk function, $F(R)$:

$$F(R) = \frac{1 - R^2}{2R} \qquad (3)$$

where R is the reflectance value of the sample. Moreover, the absorption edge values of the samples were de-
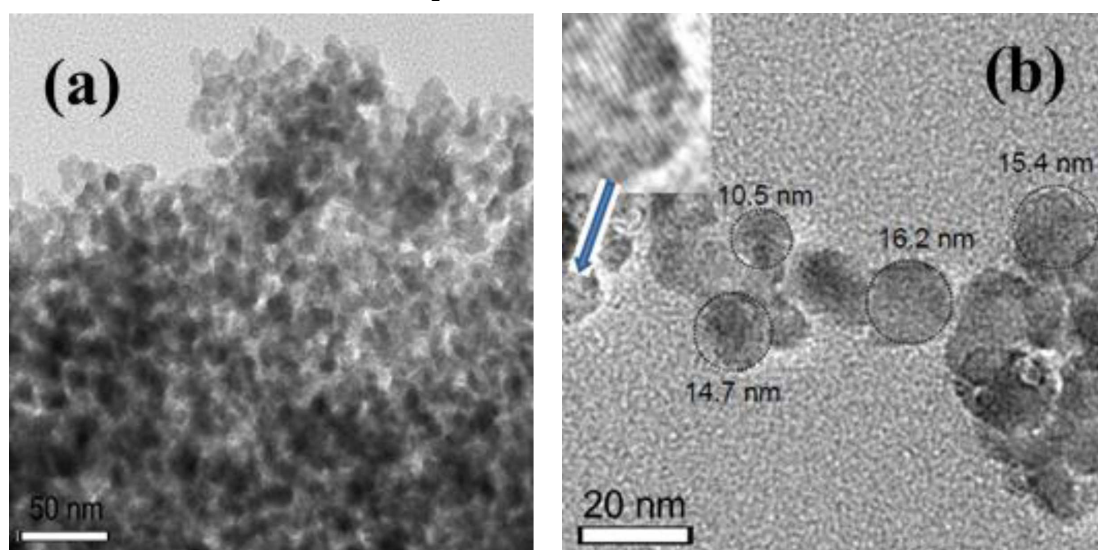
Figure 5. TEM images of the nanostructured CeO$_2$: a) bright-field and b) high resolution image
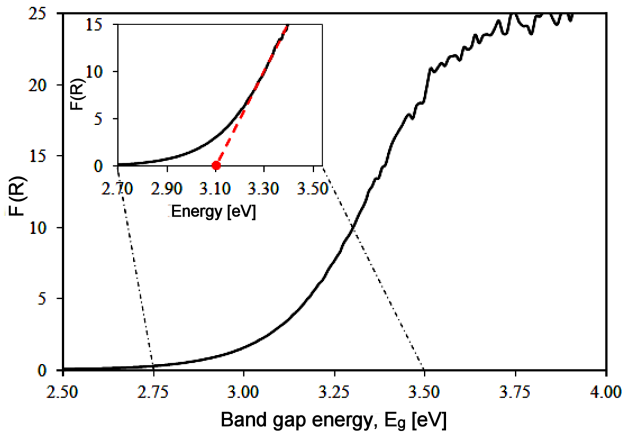
Figure 6. A plot between Kubelka-Munk function and band gap energy of the nanostructured CeO₂
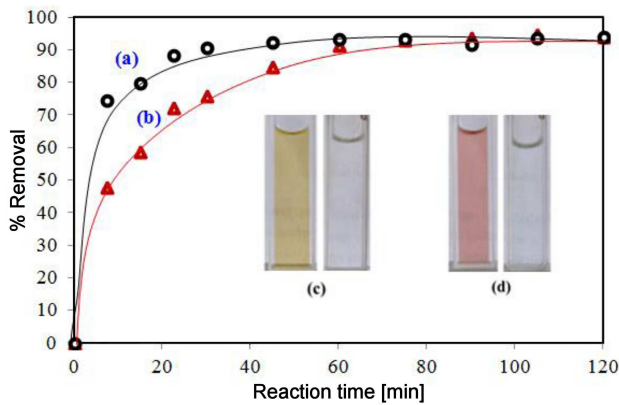
Figure 7. Time dependence on percentage adsorption of the AO-10 (a), and CR (b) (inset: colour change of AO-10 solution (c) and CR solution (d) after 0 min (left) and 60 min (rigth) of reaction time)

termined by plotting between the K-M function, $F(R)$, and band gap energy (E_g) as shown in Fig. 6. It can be

seen from Fig. 6, the band gap energy of the CeO_2 was found to be about 3.1 eV.

One of the main applications of metal oxide-based nanomaterial in the field of environmental protection and remediation is for the removal of synthetic dye pollutants. In this study, to evaluate the property of the nanostructured CeO_2 as an adsorbent, the adsorption testing was conducted with AO-10 and CR synthetic dyes. Figure 7 shows the percentage adsorption of AO-10 and CR dyes on the nanostructured CeO_2. Using AO-10 dye as the adsorbate (Fig. 7a), the adsorption rate was found increase rapidly within the first 7.5 min and then moderately. Very small increase of the adsorption rate can be observed after 30 min, indicating that the equilibrium has been achieved. In the case of CR dye as the adsorbate (Fig. 7b), the trend of the adsorption curve was difference compared to the AO-10. The rate of the CR adsorption was found to be lower than AO-10 within the first 7.5 min and continue increase during the course of reaction. No equilibrium adsorption can be observed until 60 min of reaction time. On the other hand, the adsorption process of the CR dyes still occurs, implying that longer time is required to achieve its equilibrium; thus, the absorption process was extent to 120 min. From Fig. 7, it was estimated that the adsorption equilibrium for AO-10 and CR might be occurred at 60 and 90 min of reaction time, respectively, giving a percentage removal of 96.82 % for AO-10 dye and 93.55 % for CR dye. The adsorption of both AO-10 and CR dyes can also be visually observed through the colour change of the tested dye solutions as shown in inset of Fig. 7. Both dye tested solutions changed from coloured to a clear solutions (inset of Fig. 7), which correspondence to decrease in the UV-Vis absorbance of the dye tested solutions as presented in Fig. 8.

Figure 9 presents FTIR spectra of the nanostructured CeO_2 powder before and after used as adsorbent for AO-

(a)

(b)
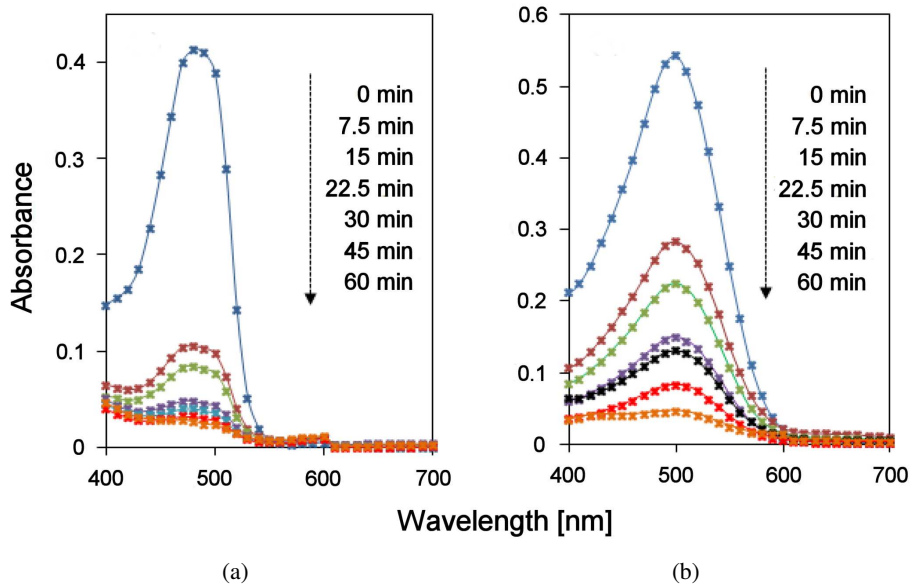
Figure 8. UV-Vis spectra evolution of: a) AO-10 and b) CR treated solution measured at certain interval time within the first 60 min of reaction time
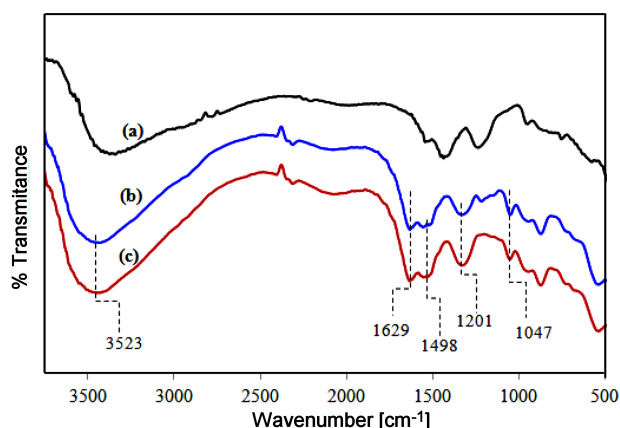
Figure 9. FT-IR spectra of CeO₂ powder: a) before, b) after its use for AO-10 adsorption, and c) after its use for CR adsorption for 120 min of reaction time

10 and CR dyes adsorption. FTIR spectra of the CeO_2 powder after adsorption of AO-10 (Fig. 9b) showed some obvious additional peaks which are not present in the CeO_2 powder before its application for adsorption (Fig. 9a). Thus, in Fig. 9b, peaks at 3523, 1629, 1498, 1201 and 1047 cm^{-1} can be seen, and these points correspond to OH stretching vibration, –C=C– stretching, –N=N– stretching vibration, –C–N– symmetric and asymmetric stretching, respectively [39]. However, all these characteristic peaks of azo dye [40] were absent in the CeO_2 before adsorption (Fig. 9a), indicating that the AO-10 was absorbed on the CeO_2. Not surprisingly, similar peaks positions of azo type dyes are found in the CeO_2 powder after its use for CR dye adsorption (Fig. 9c). This confirms that functional groups of azo type dyes are dominant; thus the different between CeO_2 before and after adsorption can be easily observed. In addition, the adsorption of the AO-10 and CR dyes on the CeO_2 is also evident from a comparison of the colour of the CeO_2 before (Fig. 10a) and after adsorption (Figs. 10b,c). It can be seen that the colour of the CeO_2 after AO-10 adsorption (Fig. 10b) is comparable to that of AO-10 dye solution (inset of Fig. 10b). A similar observation was found for the CeO_2 after its use for CR dye adsorption (inset of Fig. 10c).

Moreover, the FTIR data can be used to prove by which the CeO_2 might be acted as adsorbed for the azo dyes (AO-10 and CR dyes) rather than as a catalyst. However, a further study is highly required to confirm the adsorption phenomenon.

IV. Conclusions

High purity of nanostructured CeO_2 powder having crystal phase of face centered cubic (*fcc*) with good crystalline nature has been synthesized using a simple precipitation method with cerium nitrate compound as precursor. Evaluation of adsorption performance demonstrated that the nanostructured CeO_2 can rapidly adsorb the AO-10 and CR dyes. For 1 h adsorption time, it is clear that the adsorption activity of the nanostructured CeO_2 was higher for the AO-10 dyes adsorption than that of the CR dye. Based on the result of this study, it can be concluded that the nanostructured CeO_2 is promising for the removal of synthetic dyes in aqueous solution. In addition, understanding the kinetic, equilibrium and thermodynamic of the dyes adsorption procesess are recommended for our further studies.

References

1. M. Llusar, L. Vitaskova, P. Sulcova, M.A. Tena, J.A. Badenes, G. Monros, "Red ceramic pigments of terbium-doped ceria prepared through classical and non-conventional coprecipitation routes", *J. Eur. Ceram. Soc.*, **30** [3] (2010) 37–52.

2. H. Abimanyu, B.S. Ahn, C.S. Kim, K.S. Yoo, "Preparation and characterization of MgO-CeO₂ mixed oxide catalysts by modified coprecipitation using ionic liquids for dimethyl carbonate synthesis", *Ind. Eng. Chem. Res.*, **46** [24] (2007) 7936–7941.

3. R.X. Li, S. Yabe, M. Yamashita, S. Momose, S.

Figure 10. Digital photograph of : (a) powdered CeO₂ before used, (b) powdered CeO₂ after used for AO-10 adsorption (inset 15 mg/l of AO-10 dye solution), and (c) powdered CeO₂ after used for CR adsorption (inset 15 mg/l of CR dye solution) for 120 min of reaction time

Yoshida, S. Yin, "Synthesis and UV-shielding properties of ZnO- and CaO-doped CeO_2 via soft solution chemical process", *Solid State Ionics*, **51** (2002) 235–241.

4. S. Yabe, T. Sato, "Cerium oxide for sunscreen cosmetics", *J. Solid State Chem.*, **171** (2003) 7–11.

5. A. Corma, P. Atienzar, H. Garcıa, J.Y. Chane-Ching, "Hierarchically mesostructured doped CeO_2 with potential for solar-cell use", *Nat. Mater.*, **3** [6] (2004) 394–397.

6. E.P. Murray, T. Tsai, S.A. Barnett, "A direct-methane fuel cell with a ceria-based anode", *Nature*, **400** (1999) 649–651.

7. J.H. Song, M.G. Jung, H.W. Park, H.T. Lim, "The Effect of fabrication conditions for GDC buffer layer on electrochemical performance of solid oxide fuel cells", *Nano-Micro Lett.*, **5** [3] (2013) 151–158.

8. B.S. Liu, X.J. Zhao, N.Z. Zhang, Q.N. Zhao, X. He, J.Y. Feng, "Photocatalytic mechanism of TiO_2-CeO_2 films prepared by magnetron sputtering under UV and visible light", *Surf. Sci.*, **595** [1-3] (2005) 203–211.

9. M.G. Sanchez, J.L. Gazquez, "Oxygen vacancy model in strong metal-support interaction", *J. Catal.*, **104** (1987) 120–135.

10. X. Ouyang, W. Li, S. Xie, T. Zhai, M. Yu, J. Gan, X. Lu, "Hierarchical CeO_2 nanospheres as highly-efficient adsorbents for dye removal", *New J. Chem.*, **37** (2013) 585–588.

11. P. Ji, J. Zhang, F. Chen, M. Anpo, "Study of adsorption and degradation of acid orange 7 on the surface of CeO_2 under visible light irradiation", *Appl. Catal. B: Environ.*, **85** (2009) 148–154.

12. D. Sun, M. Gu, R. Li, S. Yin, X. Song, B. Zhao, C. Li, J. Li, J. Feng, T. Sato, "Effects of nitrogen content in monocrystalline nano-CeO_2 on the degradation of dye in indoor lighting", *Appl. Surf. Sci.*, **280** (2013) 693–697.

13. E. Matijević, W.P. Hsu, "Preparation and properties of monodispersed colloidal particles of lanthanide compounds: I. gadolinium, europium, terbium, samarium, and cerium(III)", *Colloid. Interf. Sci.*, **118** (1987) 506–523.

14. H. Yang, C. Huang, A. Tang, X. Zhang, W. Yang, "Microwave assisted synthesis of ceria nanoparticles", *Mater. Res. Bull.*, **40** (2005) 1690–1695.

15. Y. Öztürk, M. Erol, E. Çelik, O. Mermer, G. Kahraman, I. Avgýn, "Structural and magnetic properties of cerium-doped yttrium-iron garnet thin films prepared on different substrates using the sol-gel process", *Mater. Technol.*, **74** (2013) 59–63.

16. J.J. Miao, H. Wang, Y.R. Li, J.M. Zhu, J.J. Zhu, "Ultrasonic-induced synthesis of CeO_2 nanotubes", *J. Crystal Growth*, **281** (2005) 525–529.

17. K. Kaneko, K. Inoke, B. Freitag, "Structural and morphological characterization of cerium oxide nanocrystals prepared by hydrothermal synthesis", *Nano Lett.*, **7** (2007) 421–425.

18. S. Phokha, S. Pinitsoontorn, S. Maensiri, "Structure and magnetic properties of monodisperse Fe^{3+}-doped CeO_2 nanospheres", *Nano-Micro Lett.*, **5** (2013) 223–233.

19. H.I. Chen, H.Y. Chang, "Synthesis of nanocrystalline cerium oxide particles by the precipitation method", *Ceram. Int.*, **31** (2005) 795–802.

20. A. Bumajdad, M.I. Zaki, J. Eastoe, L. Pasupulety, "Microemulsion-based synthesis of CeO_2 powders with high surface area and high-temperature stabilities", *Langmuir*, **20** (2004) 11223–11233.

21. M.S. Priya, K. Divyashree, C. Goswami, M.L. Prabha, A.K.S. Babu, "Bioremediation of textile dyes by white rot fungi isolated from western ghats area", *Int. J. Eng. Adv. Tech.*, **2** (2013) 913–918.

22. S.P. Pavanelli, G.L. Bispo, C.C. Nascentes, R. Augusti, "Degradation of food dyes by zero-valent metals exposed to ultrasonic irradiation in water medium: optimization and electrospray ionization mass spectrometry monitoring", *J. Braz. Chem. Soc.*, **22** (2011) 111–119.

23. G. Annadurai, R.S. Juang, D.J. Lee, "Use of cellulose-based wastes for adsorption of dyes from aqueous solutions", *J. Hazard. Mater.*, **B92** (2002) 263–274.

24. O. Ibrahim, R. Odoh, N.J. Onyebuchi, "Effect of industrial effluent on the surrounding environment", *Archives Appl. Sci. Res.*, **4** (2012) 406–413.

25. M.G. Rusal, I. Faisal, K.M.M. Kamal, "Environmental pollution generated from process industries in Bangladesh", *J. Environ. Pollut.*, **28** [2] (2006) 144–161.

26. C. Namasivayam, R. Radhika, S. Suba, "Uptake of dyes by a promising locally available agricultural solid waste: Coir pith", *Waste Manage.*, **21** (2001) 381–387.

27. C. Hariharan, "Photocatalytic degradation of organic contaminants in water by ZnO nanoparticles", *Appl. Catal. A: General*, **304** (2006) 55–61.

28. Q.L. Sun, L.Z. Yang, "The adsorption of basic dyes from aqueous solution on modified peat-resin particle", *Water Res.*, **37** (2003) 1535–1544.

29. M.J. Prival, V.D. Mitchell, "Analysis of a method for testing azo dyes for mutagenic activity in Salmonella typhimurium in the presence of flavin mononucleotide and hamster liver S9", *Mutat. Res. - Environ. Mutat.*, **97** (1982) 103–116.

30. P. Nigam, I.M. Banat, D. Singh, R. Marchant, "Microbial process for decolorization of textile effluent

containing azo, diazo and reactive dyes", *Process Biochem.*, **31** (1996) 435–442.

31. P. Pandit, S. Basu, "Dye and solvent recovery in solvent extraction using reverse micelles for the removal of ionic dyes", *Ind. Eng. Chem. Res.*, **43** (2004) 7861–7864.

32. O. Zuas, N. Hamim, "Synthesis, Characterization and Properties of CeO$_2$-doped TiO$_2$ Composite Nanocrystals", *Mater. Sci. (Medziagotyra)*, **19** [4] (2013) 443–447.

33. M. García-hernández, M. Chadeyron, D. Boyer, A. García-murillo, F. Carrilloromo, R. Mahiou, "Hydrothermal synthesis and characterization of europium-doped barium titanate nanocrystallites", *Nano-Micro Lett.*, **5** (2013) 57–65.

34. Y.D. Wang, C.L. Ma, X.D. Sun, H.D. Li, "Preparation of nanocrystalline metal oxide powders with the surfactant-mediated method", *Inorg. Chem. Commun.*, **5** (2002) 751–755.

35. M.M. Mohamed, W.A. Bayoumy, M. Khairy, M.A. Mousa, "Synthesis of micro–mesoporous TiO$_2$ materials assembled via cationic surfactants: Morphology, thermal stability and surface acidity character-

istics", *Micropor. Mesopor. Mater.*, **103** (2007) 174–183.

36. E. Kumar, P. Selvarajan, K. Balasubramanian, "Preparation and studies of cerium cioxide nanoparticle by microwave-assisted solution method", *Rec. Res. Sci. Technol.*, **2** (2010) 37–41.

37. S. Phoka, P. Laokul, E. Swatsitang, V. Promarak, S. Seraphin, S. Maensiri, "Synthesis, structural and optical properties of CeO$_2$ nanoparticles synthesized by a simple polyvinyl pyrrolidone (PVP) solution route", *Mater. Chem. Phys.*, **115** (2009) 423–428.

38. S.N. Karthick, K. Prabakar, A. Subramania, J.T. Hong, J.J. Jang, H.J. Kim, "Formation of anatase TiO$_2$ nanoparticles by simple polymer gel technique and their properties", *Powder Technol.*, **205** (2010) 36–41.

39. A. Tripathi, S.K. Srivastava, "Ecofriendly treatment of azo dyes: biodecolorization using bacterial srains", *Int. J. Biosci. Biochem. Bioinform.*, **1** (2011) 37–40.

40. D.M. Srinivas, D.P. Suhagi, S. Rakesh, B. Nikhil, "Isolation and identification of bacterial culture for azo dye degrading capability", *Int. J. Res. Chem. Environ.*, **2** (2012) 69–79.